

The Current Carried by Bound States of a Superconducting Vortex

D. Rainer^a, J. A. Sauls^b and D. Waxman^c

^a*Physikalisches Institut, Universität Bayreuth, D-95440 Bayreuth, Germany*

^b*Department of Physics and Astronomy, Northwestern University, Evanston, Illinois, USA*

^c*School of Mathematical and Physical Sciences, The University of Sussex, Brighton BN1 9QH, Sussex, England*

(submitted April 17, 1996)

We calculate the spectrum of quasiparticle excitations in the core of isolated pancake vortices in clean layered superconductors. We show that both the circular current around the vortex center as well as any transport current through the vortex core is carried by localized states bound to the core by Andreev scattering. Hence the physical properties of the core are governed in clean high- κ superconductors (e.g. the cuprate superconductors) by the Andreev bound states, and not by normal electrons as it is the case for traditional (dirty) high- κ superconductors.

I. INTRODUCTION

We discuss specific aspects of the core of a vortex line in layered high T_c superconductors. The physics of these vortices is governed by two distinct length scales, the London penetration depth in the planes, $\lambda_{\parallel} \approx 10^3 \text{ \AA}$, and the coherence length in the planes, $\xi_{\parallel} \approx 10 - 20 \text{ \AA}$. The penetration depth is the electromagnetic length scale of a vortex. The physics on this length scale is well described by a combination of macroscopic electromagnetism, London's theory for supercurrents along the layers, and interlayer Josephson coupling. This description breaks down in the core of the vortex, *i.e.* at distances of order ξ_{\parallel} from the center of the vortex. Thus, physical properties of the core carry information on the microscopic physics of high T_c superconductivity. The small coherence length of high T_c superconductors makes the vortex core a good potential sensor for microscopic mechanisms of superconductivity. Our discussion of the vortex core in high T_c superconductors is based on the Fermi-liquid model of superconductivity. The physical properties of the vortex core predicted by this model are spectacular, unique, and could serve as fingerprints of the traditional pairing theory of superconductivity.

The vortex core of traditional high- κ superconductors is well described by the Bardeen-Stephen model¹ which represents the core by a region of normal electrons. The Bardeen-Stephen model is justified as long as the mean free path, ℓ , is much shorter than the core size, so that the motion of an electron gets randomized before it leaves the core. This condition is not fulfilled in high T_c superconductors which are generally clean superconductors with $\ell > \xi_{\parallel}$. The core of a vortex in a clean superconductor was first studied in the classic papers of Caroli, Matricon, and de Gennes.^{2,3} These authors calculated the spectrum of quasiparticle states in the core, and showed that electrons and holes form bound states at energies below the bulk energy gap. Further early studies of the excitation spectrum in the core can be found in Refs. 4,5.

More recent theoretical work was stimulated by the direct observation of core states in $NbSe_2$ by scanning tunnelling spectroscopy (STS).^{6,7} The recent report of STS in YBCO^{8,9} provides new information on the excitation spectrum of vortices in the high T_c cuprates. Consequently, theoretical efforts focused on the tunnelling density of states of bound states in isolated vortices and vortex lattices.¹⁰⁻¹⁶ These calculations show that the bound states in the core have a different nature compared with the usual quantum mechanical bound states in a potential well. The core states are coherent superpositions of particle states and hole states and are formed by repeated Andreev scattering from the pair potential (order parameter) in the core. Andreev scattering is a process of "retroreflection" of excitations: spatial variations of the amplitude or the phase of the order parameter induce branch conversion of electron-like excitations into hole-like excitations, and vice versa. Bound states occur at energies at which the phases of multiply reflected electron-like and hole-like states interfere constructively. The charge current carried by an incoming electron and an outgoing Andreev reflected hole is identical because the reversal of the velocity in an Andreev reflection process is compensated by the reversal of the charge due to electron-hole conversion. Consequently, Andreev bound states can transport a charge current, unlike bound states in a potential well. Charge conservation requires that the current carried by the bound states inside the core is transported outside the core by bulk supercurrents. This leads to an interplay between supercurrents flowing past the core and the bound states in the core. Hence, the physics of the 'normal core' in clean superconductors is basically the physics of the bound states in contact and intimate exchange with the superconducting environment outside the core.

Consider a stack of "pancake" vortices forming an isolated vortex line whose axis is oriented perpendicular to

the layers. We investigate the current distribution in the core of a pancake vortex, and show how this distribution changes if the vortex is exposed to a bulk supercurrent, or the circulation is changed from 2π to 4π . We calculate the *spectral current density*, which carries the information on the contribution of the states in a given energy interval to the total current density. A supercurrent in homogeneous superconductors is distributed over all continuum states. These states exhibit Doppler shifts of their energies, $\delta\epsilon = \mathbf{v}_f \cdot \mathbf{p}_s$, in the presence of a phase gradient in the order parameter (or superfluid momentum, $\mathbf{p}_s = \frac{\hbar}{2}\nabla\chi - \frac{e}{c}\mathbf{A}$). The total current is obtained by adding the contributions of states with positive shifts from quasiparticles co-moving with the flow and the contributions with negative shifts from quasiparticles that are counter-moving relative to the flow field. We find that the currents in the core have a very different spectral distribution from bulk supercurrents. The continuum states (scattering states) show smeared out Doppler shifts, and contribute very little to the total current. The dominant contributions to the circulating currents around the vortex center, as well as the currents through the core, come from Andreev bound states. Hence, the physics of vortex cores in clean superconductors ($\xi_{\parallel} \ll \ell$) is very different from the physics of the vortex core in a dirty superconductor ($\ell \ll \xi_{\parallel}$), which is well described by a continuum of normal electronic states. The calculations presented in this paper concentrate on stationary properties of the vortex core of clean layered superconductors. We expect more spectacular effects in the dynamic properties. The bound states react sensitively to the environment outside of the core. This leads to a coupling of the collective degrees of freedom in the London range of the vortex and the bound states in the core, which will produce a rich spectrum of largely unexplored dynamical phenomena.

Below we present analytical and numerical calculations for the states in the vortex core. We use two versions of a quasiclassical formulation of the BCS theory of superconductivity: a) *Andreev's theory*¹⁷ which represents the quasiclassical limit of Bogolyubov's equations,¹⁸ and b) the *quasiclassical theory* of Eilenberger¹⁹, Larkin, and Ovchinnikov²⁰ which represents the quasiclassical limit of Gorkov's Green's function theory. Andreev's theory and the quasiclassical theory are essentially equivalent for clean superconductors, and in this limit the choice of approach is largely a matter of taste. However, the quasiclassical theory has a wider range of application. It is the generalization of Landau's Fermi liquid theory to the superconducting state, and is capable of describing a broader range of superconducting materials and phenomena, such as dirty superconductors or superconductors with short inelastic lifetimes (strong-coupling superconductors).²¹ Section II contains analytical results for the bound states and the spectral current density for a pancake vortex with a superimposed bulk supercurrent. These results are obtained from Andreev's Hamiltonian¹⁷ by the methods described in Ref. 22. In section III we discuss the numerical results, which are obtained using the quasiclassical theory of Fermi-liquid superconductivity. We solve the quasiclassical transport equations to obtain self-consistently the pair amplitude (order parameter) for pancake vortices. Given the pair amplitude we calculate the excitation spectrum in the core of the vortex, and deduce from it the spectral current density. The numerical calculations are done for layered superconductors with s-wave pairing. The analytical and numerical results confirm and complement each other, and they establish the important role of the bound states for the currents in the core region of a vortex.

II. ANALYTICAL RESULTS

In this section, we investigate the spectrum of current carrying states of a two-dimensional pancake vortex in equilibrium at temperature T , in the presence of an externally imposed supercurrent. We ignore the spin degree of freedom of a quasiparticle excitation,²³ in this case it is sufficient to work in the two-dimensional space of particle-hole degrees of freedom. Operators in this space are 2×2 matrices, and we use the notation $\hat{\tau}_1, \hat{\tau}_2, \hat{\tau}_3$, for the three Pauli matrices in particle-hole space (Nambu space), and $\hat{1}$ for the unit matrix. The Hamiltonian for the quasiparticle excitations,²⁴ the Bogolyubov Hamiltonian, then reads:

$$\hat{H}_B = h_0(\hat{\mathbf{p}} + \frac{e}{c}\mathbf{A}(\hat{\mathbf{r}}))\hat{\tau}_3 + \hat{\Delta}(\hat{\mathbf{r}}), \quad h_0(\mathbf{p}) = \left(\frac{\mathbf{p}^2 - p_f^2}{2m} \right), \quad (1)$$

where $\hat{\mathbf{p}} = (\hat{p}_x, \hat{p}_y)$ and $\hat{\mathbf{r}} = (\hat{x}, \hat{y})$ are the momentum and position operators appropriate to a particle moving in two dimensions, $p_f \equiv mv_f$ is the Fermi momentum and \mathbf{A} is the electromagnetic vector potential. The order parameter, $\hat{\Delta}(\mathbf{r})$ is an off-diagonal matrix and is generally represented by a linear combination of $\hat{\tau}_1$ and $\hat{\tau}_2$.

In the absence of an externally imposed supercurrent, we write the order parameter of the vortex as

$$\Delta_0(\mathbf{r}) = \Delta_0 F(r)\hat{\tau}_1 \exp(i\varphi\hat{\tau}_3), \quad (2)$$

where Δ_0 is the magnitude of the order-parameter of a bulk superconductor at temperature T , $F(r)$ is the normalized profile of the vortex, which is a monotonically increasing function of r obeying $F(0) = 0$, $F(\infty) = 1$, and φ is the

angular coordinate of \mathbf{r} with $x = r \cos \varphi$, $y = r \sin \varphi$. The main assumption we make in this section is that the order-parameter in the presence of a superflow $\mathbf{p}_s = \hbar/2 \nabla \chi - e/c \mathbf{A}$ has the form

$$\hat{\Delta}(\mathbf{r}) = \exp(+\frac{i}{2} \nabla \chi \cdot \mathbf{r} \hat{\tau}_3) \hat{\Delta}_0(\mathbf{r}) \exp(-\frac{i}{2} \nabla \chi \cdot \mathbf{r} \hat{\tau}_3) \quad (3)$$

We assume throughout this section that p_s is small compared to the bulk critical current, $v_f p_s \ll \Delta_0$.

The principal physical quantities with which we shall concern ourselves are the *spectral current density*, and the total equilibrium current density which is related to $\mathbf{j}(\mathbf{r}, \epsilon)$ by

$$\mathbf{j}(\mathbf{r}, T) = \int d\epsilon \mathbf{j}(\mathbf{r}, \epsilon) f(\epsilon), \quad f(\epsilon) = \frac{1}{\exp(\epsilon/T) + 1}. \quad (4)$$

We shall also make reference to the local density of states, $N(\mathbf{r}, \epsilon)$. The quantities $\mathbf{j}(\mathbf{r}, \epsilon)$ and $N(\mathbf{r}, \epsilon)$ may be expressed in terms of the one-particle Greens function, $1/(\epsilon - \hat{H}_B)$ or, equivalently, the ‘‘spectral function’’ $\delta(\epsilon - \hat{H}_B)$. Using the spectral function, we find that in Dirac notation,

$$\mathbf{j}(\mathbf{r}, \epsilon) = 2e \langle \mathbf{r} | \{ \frac{\hat{\mathbf{p}} + \frac{e}{c} \mathbf{A}}{2m}, \delta(\epsilon - \hat{H}_B) \} | \mathbf{r} \rangle_{1,1}, \quad (5)$$

$$N(\mathbf{r}, \epsilon) = 2 \langle \mathbf{r} | \delta(\epsilon - \hat{H}_B) | \mathbf{r} \rangle_{1,1}, \quad (6)$$

where the subscript 1, 1 denotes the upper left element of the 2×2 matrices, thereby selecting out the *particle sector* of the spectral function and the factor 2 takes into account both spin projections of the quasiparticles.

A. Andreev Hamiltonian

Most calculations of the properties of superconductors with inhomogeneous order parameters are simpler in the quasiclassical limit, where one takes advantage of the separation in the scales of the wavelength of quasiparticles near the Fermi energy and the characteristic scale for spatial variations of the pair potential, i.e. $\hbar/p_f \ll \xi_0$. The quasiclassical limit of the Bogolyubov Hamiltonian (1) is the Andreev Hamiltonian in which the kinetic energy in (1) is replaced by an operator that is *linear* in the gradient.¹⁷ Let us define the normal-state density of states at the Fermi level, $N_f = p_f/2\pi v_f$, and introduce the directions, $\hat{\mathbf{k}} = (\cos \varphi_k, \sin \varphi_k)$ and $\hat{\mathbf{l}} = (-\sin \varphi_k, \cos \varphi_k)$, which are, respectively, parallel and perpendicular to trajectories of a quasiparticle wavepacket in the quasiclassical description, i.e. $\mathbf{v}_f = v_f \hat{\mathbf{k}}$. The coordinates along these directions are defined by $\mathbf{r} = \zeta \hat{\mathbf{k}} + \eta \hat{\mathbf{l}}$. In addition we work in the limit $\lambda/\xi \gg 1$, in which case the vector potential is approximately constant in the vicinity of the vortex core and can be neglected. The order parameter in (3) can be written as

$$\hat{\Delta}(\mathbf{r}) = \Delta_0 F(r) \hat{U} \frac{(\hat{\tau}_1 \zeta + \hat{\tau}_2 \eta)}{r} \hat{U}^\dagger, \quad \hat{U} = \exp \left[+i \mathbf{p}_s \cdot \hat{\mathbf{k}} \zeta \hat{\tau}_3 \right]. \quad (7)$$

By performing a gauge transformation that removes the factor of \hat{U} in Eq. (7) we obtain the spectral current density and the local density of states in terms of the Andreev Hamiltonian for an isolated vortex,

$$\hat{H}_A = v_f \hat{p}_\zeta \hat{\tau}_3 + \Delta_0 \frac{F(\hat{r})}{\hat{r}} (\hat{\tau}_1 \hat{\zeta} + \hat{\tau}_2 \eta), \quad (8)$$

$$\mathbf{j}(\mathbf{r}, \epsilon) \simeq 4\pi e v_f^2 N_f \int_0^{2\pi} \frac{d\varphi_k}{2\pi} \hat{\mathbf{k}} \langle \zeta | \delta(\epsilon - [\hat{H}_A + v_f \mathbf{p}_s \cdot \hat{\mathbf{k}}]) | \zeta \rangle_{1,1}, \quad (9)$$

$$N(\mathbf{r}, \epsilon) \simeq 4\pi v_f N_f \int_0^{2\pi} \frac{d\varphi_k}{2\pi} \langle \zeta | \delta(\epsilon - [\hat{H}_A + v_f \mathbf{p}_s \cdot \hat{\mathbf{k}}]) | \zeta \rangle_{1,1}, \quad (10)$$

where $|\zeta\rangle$ is an eigenvector of the ‘‘one-dimensional’’ trajectory coordinate operator, $\hat{\zeta}$: $\hat{\zeta}|\zeta\rangle = \zeta|\zeta\rangle$. The operators $\hat{\zeta}$ and $\hat{\mathbf{k}} \cdot \hat{\mathbf{p}} = \hat{p}_\zeta$ appearing in \hat{H}_A are canonically conjugate: $[\hat{\zeta}, \hat{p}_\zeta] = i\hbar$. The quasiclassical interpretation given to (8) is as follows: quantum-mechanical evolution in particle-hole space takes place along classical trajectories parallel to $\hat{\mathbf{k}}$ having a fixed value of $\eta \equiv \hat{\mathbf{l}} \cdot \mathbf{r}$. Thus, η is identified as a c-number impact parameter.²⁵

B. The current density of a vortex in a flow field

Let us write the current density at temperature T as

$$\mathbf{j}(\mathbf{r}, T) = \int_{-\Lambda}^{\infty} d\epsilon \mathbf{j}(\epsilon, \mathbf{r}) f(\epsilon), \quad (11)$$

where Λ is a high energy cutoff that serves to make manipulations of $\mathbf{j}(\mathbf{r}, T)$ well defined; large positive energies are automatically cut off by the Fermi function, $f(\epsilon)$. Where no ambiguity arises, we shall take $\Lambda = \infty$. Defining $\mathbf{q} = v_f \mathbf{p}_s$, and using (8) we have

$$\mathbf{j}(\mathbf{r}, T) = 4\pi e v_f^2 N_f \int_0^{2\pi} \frac{d\varphi_k}{2\pi} \int_{-\Lambda - \mathbf{q} \cdot \hat{\mathbf{k}}}^{\infty} d\epsilon \hat{\mathbf{k}} \langle \zeta | \delta(\epsilon - \hat{H}_A) | \zeta \rangle_{1,1} f(\epsilon + \mathbf{q} \cdot \hat{\mathbf{k}}). \quad (12)$$

Next, we split up the energy integrals into the following terms

$$\mathbf{j}(\mathbf{r}, T) = \mathbf{j}_1(\mathbf{r}, T) + \mathbf{j}_2(\mathbf{r}, T) + \mathbf{j}_3(\mathbf{r}, T), \quad (13)$$

$$\mathbf{j}_1(\mathbf{r}, T) = 4\pi e v_f^2 N_f \int_0^{2\pi} \frac{d\varphi_k}{2\pi} \hat{\mathbf{k}}(\mathbf{q} \cdot \hat{\mathbf{k}}) \langle \zeta | \delta(-\Lambda - \hat{H}_A) | \zeta \rangle_{1,1}, \quad (14)$$

$$\mathbf{j}_2(\mathbf{r}, T) = 4\pi e v_f^2 N_f \int_0^{2\pi} \frac{d\varphi_k}{2\pi} \int_{-\infty}^{\infty} d\epsilon \hat{\mathbf{k}} \langle \zeta | \delta(\epsilon - \hat{H}_A) | \zeta \rangle_{1,1} [f(\epsilon + \mathbf{q} \cdot \hat{\mathbf{k}}) - f(\epsilon)], \quad (15)$$

$$\mathbf{j}_3(\mathbf{r}, T) = 4\pi e v_f^2 N_f \int_0^{2\pi} \frac{d\varphi_k}{2\pi} \int_{-\Lambda}^{\infty} d\epsilon \hat{\mathbf{k}} \langle \zeta | \delta(\epsilon - \hat{H}_A) | \zeta \rangle_{1,1} f(\epsilon). \quad (16)$$

The three contributions to the current have different interpretations.

1. Since Λ is large, $\langle \zeta | \delta(-\Lambda - \hat{H}_A) | \zeta \rangle_{1,1}$ may be replaced by its high energy, normal-state limit, $1/2\pi v_f$ and

$$\mathbf{j}_1(\mathbf{r}, T) = e v_f^2 N_f \mathbf{p}_s. \quad (17)$$

This term coincides with the $T = 0$ current of a uniform superconductor.

2. The term $\mathbf{j}_2(\mathbf{r}, T)$ contributes to ‘‘backflow’’, since it always yields a current with a component in the $-\hat{\mathbf{p}}_s$ direction.²⁶ The term $\mathbf{j}_2(\mathbf{r}, T)$ contains the current carried by the bound states and also a correction to the $T = 0$ current due to the thermal breaking of pairs. To appreciate these points we look at this term in two limits, assuming $q \ll \Delta_0$. (i) For $T = 0$ we have

$$\mathbf{j}_2(\mathbf{r}, 0) = 4\pi e v_f^2 N_f \int_0^{2\pi} \frac{d\varphi_k}{2\pi} \int_0^{-\mathbf{q} \cdot \hat{\mathbf{k}}} d\epsilon \hat{\mathbf{k}} \langle \zeta | \delta(\epsilon - \hat{H}_A) | \zeta \rangle_{1,1}. \quad (18)$$

The small size of q ensures that the energy integral only selects states in the gap, thus $\mathbf{j}_2(\mathbf{r}, 0)$ only obtains contributions from the bound states. (ii) For $T \neq 0$ and assuming $\Delta_0(\mathbf{r})$ to be that of a uniform system, $\Delta_0(\mathbf{r}) = \Delta_0 \hat{\tau}_1$, we write $f(\epsilon + \mathbf{q} \cdot \hat{\mathbf{k}}) - f(\epsilon) \approx \mathbf{q} \cdot \hat{\mathbf{k}} f'(\epsilon)$ and obtain

$$\mathbf{j}_2(\mathbf{r}, T) = -e v_f^2 N_f \mathbf{p}_s \int_{-\infty}^{\infty} d\epsilon \frac{|\epsilon|}{\sqrt{\epsilon^2 - \Delta_0^2}} \Theta(\epsilon^2 - \Delta_0^2) [-f'(\epsilon)] = -e v_f^2 N_f \mathbf{p}_s Y(\beta \Delta_0), \quad (19)$$

where $Y(\beta \Delta_0)$ is the Yosida function which gives a quantitative measure of the thermal breaking of Cooper pairs.

3. The term $\mathbf{j}_3(\mathbf{r}, T)$ is independent of \mathbf{p}_s and is simply the current density of a vortex in the absence of an externally imposed supercurrent.

C. Current carrying bound states at the center of the vortex

Consider the spectral properties at the center of the vortex. For $\eta = 0$

$$\hat{H}_A \Big|_{\eta=0} = v_f \hat{p}_\zeta \hat{\tau}_3 + \Delta_0 F(\hat{\zeta}) \hat{\tau}_1, \quad (20)$$

with $F(-\hat{\zeta}) = -F(\hat{\zeta})$ accounting for the π phase change across the vortex core. This special case of the Andreev Hamiltonian is identical in form to the continuum Hamiltonian used to describe *trans*-polyacetylene containing a single topological soliton.²⁷ It is known that this Hamiltonian always has a non-degenerate bound state at zero energy.²⁸ Whether or not it has other bound states depends on the form of the profile, $F(\zeta)$. For the single quantum vortex and trajectories through the center there are no other bound states. The eigenfunction for the zero-energy bound state, $\psi_0(\zeta)$, is found by solving $\left[v_f \frac{\partial \zeta}{\partial \tau} \hat{\tau}_3 + \Delta_0 F(\zeta) \hat{\tau}_1 \right] \psi_0(\zeta) = 0$. The normalized solution is

$$\psi_0(\zeta) = \frac{1}{\sqrt{L}} \exp\left(-\frac{\Delta_0}{v_f} \int_0^\zeta d\zeta' F(\zeta')\right) \begin{pmatrix} \frac{1}{\sqrt{2}} \\ -\frac{1}{\sqrt{2}} \end{pmatrix}, \quad (21)$$

$$L = 2 \int_0^\infty d\zeta \exp\left(-\frac{2\Delta_0}{v_f} \int_0^\zeta d\zeta' F(\zeta')\right), \quad (22)$$

where L is a profile dependent quantity with the dimensions of length, $L \sim v_f/\Delta_0$. Analytical estimates of the bound states at distances far from the vortex are given in appendix IV B.

For energies $|\epsilon| < \Delta_0$ only the bound state of H_A will contribute to the spectral current density (and the local density of states),

$$\mathbf{j}(\epsilon, \mathbf{0}) \simeq 4\pi e v_f^2 N_f \int_0^{2\pi} \frac{d\varphi_k}{2\pi} \hat{\mathbf{k}} \delta(\epsilon - v_f \mathbf{p}_s \cdot \hat{\mathbf{k}}) \left[\psi_0(0) \psi_0^\dagger(0) \right]_{1,1} \quad (23)$$

$$= \left[\frac{\epsilon}{p_s} \frac{2e N_f \Delta_0}{L/\xi} \frac{\Theta((v_f p_s)^2 - \epsilon^2)}{\sqrt{(v_f p_s)^2 - \epsilon^2}} \right] \hat{\mathbf{p}}_s, \quad |\epsilon| < \Delta_0. \quad (24)$$

There is a simple relation between $\mathbf{j}(\epsilon, \mathbf{0})$ and $N(\epsilon, \mathbf{0})$ when $|\epsilon| < \Delta_0$. In (23), the delta function in the integrand of $\mathbf{j}(\epsilon, \mathbf{0})$ effectively replaces $\hat{\mathbf{k}}$ by $(\epsilon/v_f p_s) \hat{\mathbf{p}}_s$. Taking this factor outside the integral leaves an integral identical to that of the local density of states. Consequently,

$$\mathbf{j}(\epsilon, \mathbf{0}) = e \frac{\epsilon}{p_s} N(\epsilon, \mathbf{0}) \hat{\mathbf{p}}_s, \quad |\epsilon| < \Delta_0. \quad (25)$$

Note that the contribution of negative energy (bound) states to the total current density lies in the $-\hat{\mathbf{p}}_s$ direction, i.e. *opposite* to the externally imposed supercurrent. At zero temperature the total current density originates from the bound states having energies $-\Delta_0 < \epsilon < 0$,

$$\mathbf{j}_{bound}(\mathbf{0}, T=0) = \int_{-\Delta_0}^0 \mathbf{j}(\epsilon, \mathbf{0}) d\epsilon = -\frac{2e N_f \Delta_0}{L/\xi} v_f \hat{\mathbf{p}}_s. \quad (26)$$

The current density of an isolated vortex with $p_s = 0$ vanishes at the center of the vortex, i.e. $\mathbf{j}_3(\mathbf{0}, T) = 0$. We can combine the result in (26) with \mathbf{j}_1 given in (17) to obtain the total current density at $T = 0$:

$$\mathbf{j}(\mathbf{r} = \mathbf{0}, T=0) = e v_f^2 N_f \mathbf{p}_s - \frac{2N_f e \Delta_0}{L/\xi} v_f \hat{\mathbf{p}}_s. \quad (27)$$

Thus, for sufficiently small \mathbf{p}_s the bound-state contribution dominates (27) and $\mathbf{j}(\mathbf{r} = \mathbf{0}, T=0)$ will point in the $-\hat{\mathbf{p}}_s$ direction.

D. Particle conservation

For equilibrium conditions the divergence of the current density vanishes. From (17), \mathbf{j}_1 has a vanishing divergence, and for an undisturbed vortex we have $\nabla \cdot \mathbf{j}_3(\mathbf{r}) = 0$. Thus, $S(\mathbf{r}) = \nabla \cdot \mathbf{j}(\mathbf{r}) \equiv \nabla \cdot \mathbf{j}_2(\mathbf{r})$. At $T = 0$,

$$S(\mathbf{r}) = 4\pi e v_f N_f \int_0^{2\pi} \frac{d\varphi_k}{2\pi} \int_0^{-\mathbf{q} \cdot \hat{\mathbf{k}}} d\epsilon v_f \frac{\partial}{\partial \zeta} \left(\langle \zeta | \delta(\epsilon - \hat{H}_A) | \zeta \rangle_{1,1} \right). \quad (28)$$

In Eq. (49) of appendix IV A we show that

$$v_f \frac{\partial}{\partial \zeta} \langle \zeta | \delta(\epsilon - \hat{H}_A) | \zeta \rangle_{1,1} = \Delta_0 \frac{F(r)}{r} \text{tr} \left[(\zeta \hat{\tau}_2 - \eta \hat{\tau}_1) \langle \zeta | \delta(\epsilon - \hat{H}_A) | \zeta \rangle \right], \quad (29)$$

yielding

$$S(\mathbf{r}) = 4\pi e v_f \Delta_0 N_f \int_0^{2\pi} \frac{d\varphi_k}{2\pi} \int_0^{-\mathbf{q} \cdot \hat{\mathbf{k}}} d\epsilon \frac{F(r)}{r} \text{Tr} \left[(\zeta \hat{\tau}_2 - \eta \hat{\tau}_1) \langle \zeta | \delta(\epsilon - \hat{H}_A) | \zeta \rangle \right]. \quad (30)$$

Since $q \ll \Delta_0$, only the bound state, $\psi_0(\zeta; \eta)$, contributes to the ϵ integral. Thus,

$$S(\mathbf{r}) = 4\pi e v_f N_f \Delta_0 \int_0^{2\pi} \frac{d\varphi_k}{2\pi} \int_0^{-\mathbf{q} \cdot \hat{\mathbf{k}}} d\epsilon \delta(\epsilon - \epsilon_0(\eta)) \psi_0^\dagger(\zeta; \eta) \frac{F(r)}{r} (\hat{\tau}_2 \zeta - \hat{\tau}_1 \eta) \psi_0(\zeta; \eta), \quad (31)$$

where $\epsilon_0(\eta)$ is the bound-state energy for an impact parameter η . At small distances from the center of the vortex ($r \ll \xi$) $F(r) \approx r/\xi$, with $\xi \approx v_f/2\Delta_0$, and the lowest energy bound state is then

$$\psi_0(\zeta; \eta) = \frac{1}{\pi^{1/4}} \frac{1}{\sqrt{\xi}} \exp\left(-\frac{\zeta^2}{2\xi^2}\right) \begin{pmatrix} \frac{1}{\sqrt{2}} \\ -\frac{i}{\sqrt{2}} \end{pmatrix}, \quad (32)$$

$$\epsilon_0(\eta) = -\Delta_0 \frac{\eta}{\xi}. \quad (33)$$

Substituting ψ_0 and ϵ_0 into (31) and setting $\exp(-\frac{1}{2}\zeta^2/\xi^2) \approx 1$ yields

$$S(\mathbf{r}) \approx \frac{4}{\sqrt{\pi}} N_f \Delta_0^2 \frac{\frac{\mathbf{q} \cdot \mathbf{r}}{\xi}}{\left| \frac{r}{\xi} \hat{\varphi} - \frac{\mathbf{q}}{\Delta_0} \right|}, \quad (34)$$

which is non-zero, indicating that the ansatz (3) is not physically correct for any value of \mathbf{p}_s . This failure to satisfy the conservation law is due to the lack of self-consistency of the order parameter in Eq. (3) in the presence of the flow field. In the absence of pinning, the vortex will move in response to a flow field, even one of arbitrarily small strength. The results in section II implicitly assume a *pinned* vortex. Thus, there will be distortion of the vortex away from its cylindrically symmetric equilibrium form (3). In the following section we show that the self-consistently determined vortex order parameter, which includes the deformation by the flow field, restores the conservation law.

III. QUASICLASSICAL RESULTS

A versatile and efficient method for calculating local spectral properties of superconductors is the quasiclassical theory of superconductivity.^{19,20,29,30} This theory is well adapted for a numerical approach to microscopic problems in superconductivity, such as the calculation of the structure and the excitation spectrum of vortex cores for superconductors with isotropic, anisotropic or unconventional order parameters. The quasiclassical theory is the only theoretical formulation which can handle equally well clean and dirty superconductors, as well as more complicated geometries than that of an isolated vortex with cylindrical symmetry or a perfect vortex lattice. It can be interpreted as the generalization of Landau's theory of normal Fermi liquids to the superconducting state. The quasiclassical theory shares with Landau's theory the semiclassical description of the orbital degrees of freedom of quasiparticle excitations. On the other hand, the internal degrees of freedom, *i.e.* the spin and the particle-hole degrees of freedom,

are described by quantum mechanics. Quantum mechanical coherence of particle and hole excitations is the basis of all superconducting effects such as persistent supercurrents, flux quantization, Josephson effects and Andreev reflection. Here we use the quasiclassical theory for our investigations of the vortex core. Numerical work on vortices in superconductors using the quasiclassical theory started with a series of publications by Kramer, Pesch, and Watts-Tobin.^{5,31,32} More recent work includes pinning of vortices at small defects,³³ vortices in superfluid ³He and other systems with unconventional pairing,^{34,35} the excitation spectrum of bound quasiparticles,^{12,36} and the spectrum of moving pancake vortices.³⁷

We use in this article the notation of Refs. 38,39,21. The central objects of the quasiclassical theory of superconductors in equilibrium are the quasiclassical propagators $\hat{g}^{R,A}(\mathbf{p}_f, \mathbf{r}; \epsilon)$, which are 2×2 matrices in the particle-hole index,

$$\hat{g}^{R,A} = \begin{pmatrix} g^{R,A}(\mathbf{p}_f, \mathbf{r}; \epsilon) & f^{R,A}(\mathbf{p}_f, \mathbf{r}; \epsilon) \\ \underline{f}^{R,A}(\mathbf{p}_f, \mathbf{r}; \epsilon) & \underline{g}^{R,A}(\mathbf{p}_f, \mathbf{r}; \epsilon) \end{pmatrix}. \quad (35)$$

The variables ϵ and \mathbf{p}_f stand for the energy of an excitation and its momentum (on the Fermi surface). The momentum variable reduces to $\mathbf{p}_f = p_f(\cos \varphi_k, \sin \varphi_k)$ for an isotropic Fermi surface in two dimensions (see section II). General symmetries lead to the following fundamental relation between \hat{g}^R and \hat{g}^A ,

$$\hat{g}^A = \hat{\tau}_3 (\hat{g}^R)^\dagger \hat{\tau}_3. \quad (36)$$

We use, as described in Section II, the notation $\hat{\tau}_1, \hat{\tau}_2, \hat{\tau}_3$, for the three Pauli matrices in particle-hole space, and $\hat{1}$ for the unit matrix. The off-diagonal terms $f^{R,A}$ in Eq. (35) are the pair amplitudes. They vanish in the normal state, and measure the amount of particle-hole mixing in the superconducting state. The diagonal elements of the propagators determine the density of states,

$$N(\mathbf{p}_f, \mathbf{r}; \epsilon) = N_f \frac{g^R(\mathbf{p}_f, \mathbf{r}; \epsilon) - g^A(\mathbf{p}_f, \mathbf{r}; \epsilon)}{-2\pi i}, \quad (37)$$

and the equilibrium current density. The most detailed information on the current distribution is obtained from the *spectral current density*,

$$\mathbf{j}(\mathbf{p}_f, \mathbf{r}; \epsilon) = e \mathbf{v}_f N_f (\mathcal{N}_+(\mathbf{p}_f, \mathbf{r}; \epsilon) - \mathcal{N}_-(\mathbf{p}_f, \mathbf{r}; \epsilon)), \quad (38)$$

where $\mathcal{N}_\pm(\mathbf{p}_f, \mathbf{r}; \epsilon) = N(\pm \mathbf{p}_f, \mathbf{r}; \epsilon)/N_f$ is the dimensionless density of states for co-moving (+) and counter-moving (-) excitations along the trajectory line defined by \mathbf{p}_f , and \mathbf{v}_f is the Fermi velocity at the point \mathbf{p}_f on the Fermi surface. This spectral density measures the contributions of quasiparticle states with energy ϵ and momentum near the Fermi surface point \mathbf{p}_f to the current density at position \mathbf{r} . The full current density is obtained by weighting the spectrally resolved current density by the occupation probability of the quasiparticle states, then integrating over Fermi momenta and energies. For equilibrium states,

$$\mathbf{j}(\mathbf{r}) = 2 \int d\epsilon \int d\mathbf{p}_f \mathbf{j}(\mathbf{p}_f, \mathbf{r}; \epsilon) \left(f(\epsilon) - \frac{1}{2} \right), \quad (39)$$

where $f(\epsilon)$ is the Fermi distribution function. The symbol $\int d\mathbf{p}_f$ denotes a weighted integral over the Fermi surface. The weight at \mathbf{p}_f is $\propto |\mathbf{v}_f|^{-1}$, and the integral is normalized, $\int d\mathbf{p}_f 1 = 1$. The spectral current density is particularly well suited for our study of the importance of Andreev bound states for the current flow in a vortex core. These bound states appear as delta functions in the spectral current density at energies below the bulk energy gap. The spectral weight of the delta function, combined with the occupation of the bound state, determine its contribution to the total current density.

We calculate $\hat{g}^R(\mathbf{p}_f, \mathbf{r}; \epsilon)$ from Eilenberger's transport equation¹⁹

$$\left[\left(\epsilon + \frac{e}{c} \mathbf{v}_f \cdot \mathbf{A}(\mathbf{r}) \right) \hat{\tau}_3 - \hat{\Delta}(\mathbf{p}_f, \mathbf{r}), \hat{g}^R(\mathbf{p}_f, \mathbf{r}; \epsilon) \right] + i \hbar \mathbf{v}_f \cdot \nabla \hat{g}^R(\mathbf{p}_f, \mathbf{r}; \epsilon) = 0, \quad (40)$$

supplemented by the condition of analyticity in the upper half of the complex ϵ -plane, and the normalization condition

$$\hat{g}^R(\mathbf{p}_f, \mathbf{r}; \epsilon)^2 = -\pi^2 \hat{1}. \quad (41)$$

For a fixed Fermi momentum \mathbf{p}_f this is a first order differential equation along a straight-line classical trajectory in the direction of the Fermi velocity \mathbf{v}_f . The propagator $\hat{g}^R(\mathbf{p}_f, \mathbf{r}; \epsilon)$ at a chosen point of interest, \mathbf{r} , is determined by

the solution of (40) along the trajectory through \mathbf{r} in the direction \mathbf{v}_f . Complete information on the local physical properties at point \mathbf{r} , such as the current density, is obtained by sampling all trajectories through \mathbf{r} . The propagator $\hat{g}^R(\mathbf{p}_f, \mathbf{r}; \epsilon)$ is intimately related to the 2×2 density matrix of the particle-hole degrees of freedom of a quasiparticle moving along the classical trajectory specified by \mathbf{p}_f, \mathbf{r} . Thus, $\hat{g}^R(\mathbf{p}_f, \mathbf{r}; \epsilon)$ describes the state of the internal degrees of freedom of the excitation. The internal state, *i.e.* the amount of particle-hole mixing, may change along the trajectory as a consequence of the off-diagonal pair potential, $\hat{\Delta}(\mathbf{p}_f, \mathbf{r})$, which acts as a driving term that ‘rotates’ the particle-hole pseudo spin. The pair potential couples particle and hole excitations, and is the origin of particle-hole coherence. It depends on the real space position, \mathbf{r} , and, for anisotropic superconductors, on the Fermi surface position, \mathbf{p}_f ,

$$\hat{\Delta}(\mathbf{p}_f, \mathbf{r}) = \begin{pmatrix} 0 & \Delta(\mathbf{p}_f, \mathbf{r}) \\ -\Delta^*(\mathbf{p}_f, \mathbf{r}) & 0 \end{pmatrix}. \quad (42)$$

The pair potential must be calculated self-consistently from the gap equation,

$$\Delta(\mathbf{p}_f, \mathbf{r}) = \int d\mathbf{p}'_f V(\mathbf{p}_f, \mathbf{p}'_f) \int \frac{d\epsilon}{2\pi} \text{Im} f^R(\mathbf{p}'_f, \mathbf{r}; \epsilon) (1 - 2f(\epsilon)), \quad (43)$$

where $V(\mathbf{p}_f, \mathbf{p}'_f)$ is the pairing interaction, which determines the orbital symmetry of the pair potential, its magnitude and T_c .

Our procedure for numerical calculation of the currents in the core of 2D pancake vortices is the following. We first solve self-consistently the gap equation and Eilenberger’s equation at Matsubara energies. This allows us to determine the pair potential and the supercurrent density. We then insert the pair potential into Eilenberger’s differential equation at real energies, and obtain from its solution the excitation spectrum: the density of states and the spectral current density. The differential equations are solved by standard 4th order Runge-Kutta and multiple shooting methods, and self-consistency is achieved iteratively by using alternatively a relaxation method and the Möbius-Eschrig algorithm.⁴⁰

We consider three examples of pancake vortices: isolated, i) singly-quantized and ii) doubly-quantized s -wave vortices, and iii) a pinned s -wave vortex in the presence of a uniform transport supercurrent. We choose a temperature of $T = 0.4 T_c$, unless otherwise noted, and assume $\kappa = \lambda/\xi \gg 1$. In this limit the vector potential is essentially constant in the core region, and can be neglected.

A. Spectral current density of a singly-quantized s -wave vortex

Figure 1 shows the amplitude of the order parameter of a singly-quantized s -wave vortex. The amplitude is isotropic and vanishes linearly in the core. The variation of the amplitude and phase along two trajectories are also shown in Fig. 1. For trajectory a passing through the center of the vortex, the phase changes discontinuously and the amplitude vanishes linearly at the vortex center. For trajectory b , with impact parameter $\eta = 3.0\xi_0$, there is only a small change in the amplitude of Δ . For singly-quantized vortices the phase of the order parameter is the more important factor determining the spectrum of bound states.

Figure 2 shows the angle-resolved local density of states for the two trajectories shown in Fig. 1. For trajectory (a) through the center of the vortex, the spectrum shows a zero-energy bound state separated from the continuum that begins at the bulk gap. The bound state results from constructive interference of particle- and hole-like quasiparticles that undergo Andreev reflections from the vortex order parameter. This bound state corresponds to the zero angular momentum bound state found by Caroli, de Gennes and Matricon.^{2,3} A zero-energy bound state is always present for trajectories in which the order parameter is real (up to a constant phase factor) and has different signs when going to $\pm\infty$ along the trajectory.²⁸

Bound states with non-zero energies are found for trajectories with a nonzero impact parameter measured from the vortex center. These bound states correspond to the spectrum of bound states with non-zero angular momenta obtained by Caroli et al.² Figure 2b shows the spectrum for a trajectory with an impact parameter of $\eta = 4.2\xi_0$ and $\mathbf{v}_f \cdot \mathbf{p}_s(\mathbf{r}) \geq 0$ measured at the point of closest approach to the vortex center. The bound state is shifted down in energy to $\epsilon/2\pi T_c \simeq -0.22$, and the continuum states are shifted and inhomogeneously broadened by the Doppler energy, $\Delta\epsilon = \mathbf{v}_f \cdot \mathbf{p}_s(\mathbf{r})$. The spectrum near the onset at point 1 in Fig. 2b has low weight and corresponds to the continuum edge at $\epsilon = \Delta$ far from the impact point, while the peak in the spectrum at point 2 corresponds to the maximum Doppler shift, $\epsilon = \Delta + \mathbf{v}_f \cdot \mathbf{p}_s(\mathbf{R})$ at the impact point \mathbf{R} . Note the development of the BCS coherence peak as the density of states is sampled further from the vortex center.

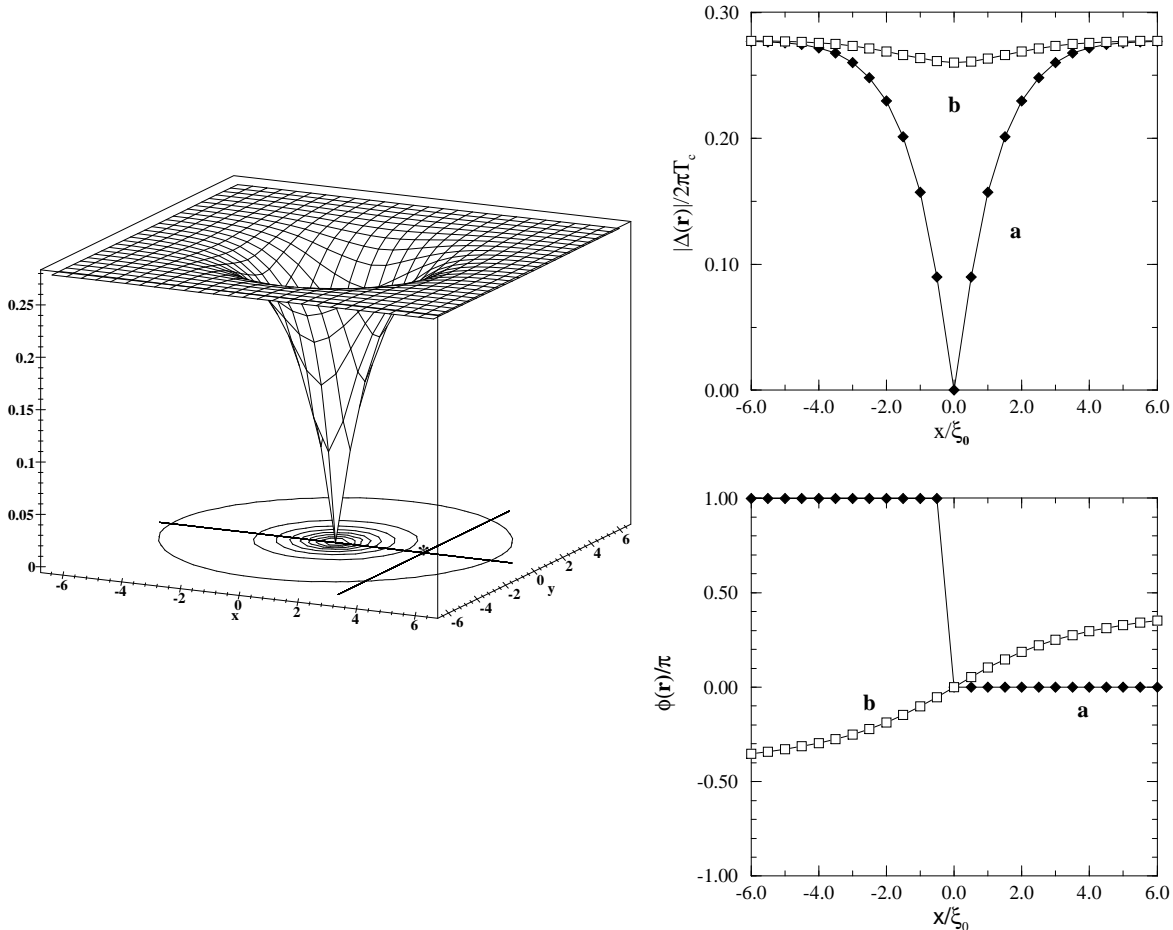


FIG. 1. The magnitude of the pair potential, $|\Delta(\mathbf{r})|/2\pi T_c$, at $T = 0.4T_c$ for a singly quantized vortex in an s -wave superconductor is shown in the 3D plot. The 2D plots show the order parameter amplitude and phase of the order parameter along a trajectory (a) passing through the center of the vortex, and (b) along a trajectory with an impact parameter of $\eta = 3.0\xi_0$. The order parameter is real along trajectory (a) and the phase changes discontinuously by π . Along trajectory (b) there is little change in amplitude, but a substantial, continuous change of phase.

The density of states of an s -wave vortices has been investigated by several authors.^{31,12,15} Our emphasis is on the importance of the Andreev bound states for the current distribution in the vortex core. We show in Fig. 2c the spectral current density for the trajectory with $\eta = 4.2\xi_0$ and $\mathbf{v}_f \cdot \mathbf{p}_s(\mathbf{r}) \geq 0$. The net current carried by the states at the point $\pm\mathbf{p}_f$ on the Fermi surface is obtained by weighting this spectrum by the equilibrium distribution and integrating over all energies. Thus, for $T \rightarrow 0$ only the negative energy states contribute. It is clear from Fig. 2c that the current in the vicinity of the vortex core is carried almost entirely by the bound states with $-|\Delta| < \epsilon < 0$. The continuum states give almost no net contribution to the current in the core. Figure 2d shows the spectral current density of the set of bound states with trajectories $\mathbf{v}_f = \pm v_f \hat{\mathbf{y}}$ as a function of the impact parameter η for $0 \leq \eta \leq 6\xi_0$. The peak at $\epsilon/2\pi T_c \simeq -0.027$ corresponds to the trajectory with impact parameter $\eta = 0.2\xi_0$. The bound state energy decreases with increasing distance from the core. For small η we obtain, $\epsilon_0(\eta) \simeq -2(\eta/\xi_0)\Delta$, in reasonable agreement

with the analytic estimate in Eq. (33). As indicated in Fig. 2d the contribution of the bound state to the current density decreases as the impact parameter increases. However, even at a relatively large distance, $\eta = 6\xi_0$, the bound state still contributes significantly to the circulating current density of the vortex.

The evolution of the bound state energy for small impact parameters can be written in terms of the angular momentum of an excitation about the vortex center, $\mathcal{L}_z = p_f \eta$; *i.e.* $\epsilon_0(\eta) = -\mathcal{L}_z \omega_0$, where $\hbar\omega_0 = 2\hbar\Delta/p_f\xi_0 \ll \Delta$. This spectrum was originally obtained by Caroli et al.² by solving the Bogolyubov equations. In the Bogolyubov or Gor'kov formulation the spectrum is discrete: $\mathcal{L}_z = (m + \frac{1}{2})\hbar$ with $m = \text{integer}$ and $\hbar\omega_0$ defining the level spacing of the low-lying bound states in the core. The lowest energy bound state in the core has a zero-point energy of $\epsilon_0 = \frac{1}{2}\hbar\omega_0 \simeq \Delta^2/E_f \ll \Delta$ which is outside the resolution of the quasiclassical or the Andreev theory. The discrete spectrum of the Bogolyubov theory corresponds to the continuous Andreev spectrum in the limit where the level spacing is small compared to all other relevant energy scales, *i.e.* $\hbar\omega_0 \ll k_B T, \hbar/\tau$, etc. This is generally an excellent approximation in conventional type II superconductors. For the high T_c cuprates the discrete level structure is expected to play a more important role, particularly in the transverse response of vortices in the ultra-clean limit, *i.e.* $\omega_0 \gg 1/\tau$, where τ is the mean scattering time.^{41,42}

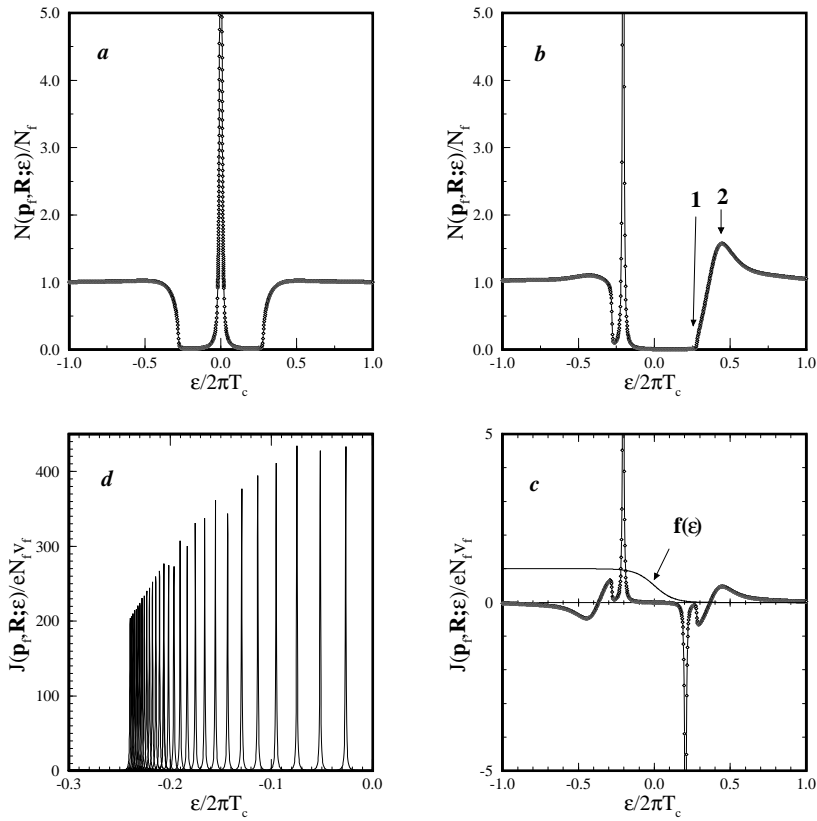


FIG. 2. *a)* Local density of states at the center of a vortex for a trajectory passing through the center of the core. The width of the bound state is set at $\gamma/2\pi T_c = 0.0004$, the continuum edge is at $\epsilon = \pm\Delta$, and the temperature is $T = 0.4T_c$. *b)* Local density of states at $\mathbf{R} = (4.2, 0)\xi_0$ for the trajectory $\mathbf{v}_f = (0, 1)v_f$. The bound state is shifted, $\epsilon/2\pi T_c \simeq -0.22$, and the continuum states show the Doppler broadening. *c)* The spectral current density for the same position and direction as in *b)*. The Fermi function for $T = 0.4T_c$ is also shown. Note that the current density is dominated by the negative energy bound state. *d)* The spectral current density for a set of parallel trajectories as a function of impact parameter for $0 < \eta < 6\xi_0$. The spatial separation between neighboring trajectories is $0.2\xi_0$.

B. Spectrum of a doubly-quantized s-wave vortex

It is interesting to compare the single-quantum vortex with the axially symmetric, 4π vortex, $\Delta(\mathbf{r}) = |\Delta(\mathbf{r})| \exp 2i\varphi$. The double quantum vortex has higher energy than a pair of isolated single-quantum vortices; however, once created the double-quantum vortex is metastable against dissociation into singly-quantized vortices. The amplitude of the order parameter for the double-quantum vortex decreases as $|\Delta(\mathbf{r})| \sim r^2$ for $r < \xi_0$ as shown in Fig. 3a.

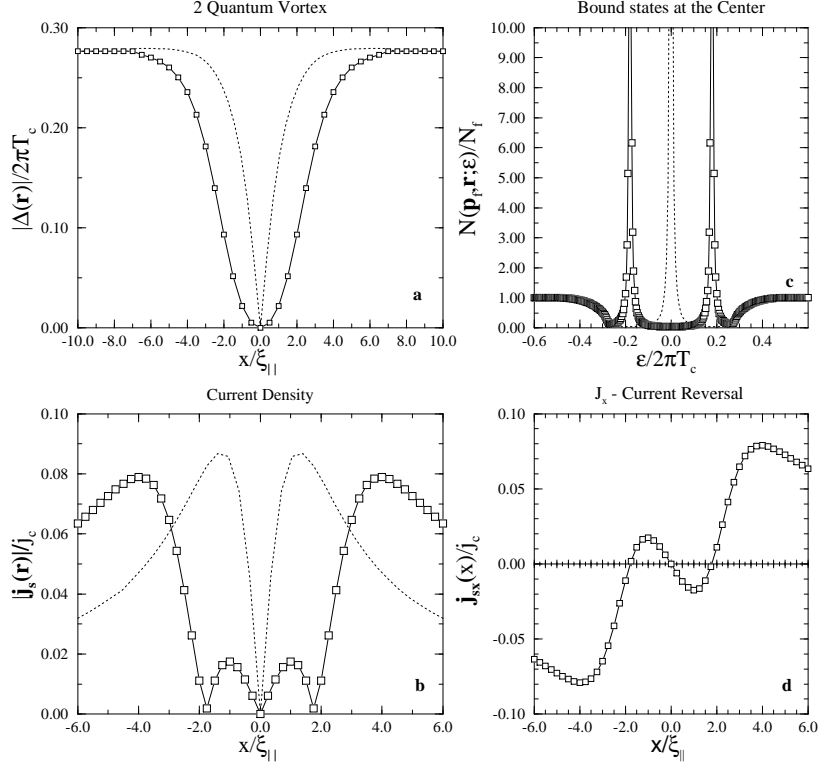


FIG. 3. a) The amplitude of the order parameter for a 4π vortex at $T = 0.4T_c$. Note the quadratic behavior for $r \ll \xi_0$. b) Local density of states at the center of the vortex for a trajectory passing through the center of the core. Two bound states are present at energies, $\epsilon/2\pi T_c = \pm 0.18$. c) The plot of $J_y(x, 0)$ vs. x shows a reversal of the direction of the current for $x < 1.9\xi_0$. d) The magnitude of the current density for the 4π vortex. The corresponding quantities for the 2π vortex are shown for comparison (dotted curves).

In contrast to the 2π vortex there is no sign change of the order parameter for trajectories passing through the center of the vortex core. This difference has a profound effect on the spectrum of Andreev bound states in the core. Fig. 3b shows the excitation spectrum of the doubly-quantized vortex at the center of a trajectory passing through the center of the vortex core. A symmetric spectrum of two bound states at $\epsilon_{\pm}/2\pi T_c = \pm 0.18$ are separated from the continuum. Figure 3 also shows the current density of the doubly-quantized vortex. The remarkable feature is the reversal of the current direction in the core, i.e. for $r \lesssim 2\xi_0$ (see Fig. 3c and 3d). This current anomaly is associated with the appearance of a counter-moving Andreev bound state below the Fermi level ($\epsilon = 0$). The evolution of the spectral current density is shown in Fig. 4. The trajectories are parallel to $\hat{\mathbf{y}}$ and the spectral current density is shown as a function of the impact parameter. At distances greater than $x \simeq 2\xi_0$ two bound states lie below zero energy, and both states are co-moving with the circulating phase gradient, \mathbf{p}_s . As the vortex core is approached the co-moving bound state nearest the Fermi level moves to higher energy, and a counter-moving bound state above the Fermi level (not shown) moves to lower energy. These two states cross the Fermi energy ($\epsilon = 0$) at approximately $x = 2\xi_0$, leading to a reversal of the integrated current density inside the core. The cumulative current density for each trajectory is shown as the thick solid line in each panel of Fig. 4.

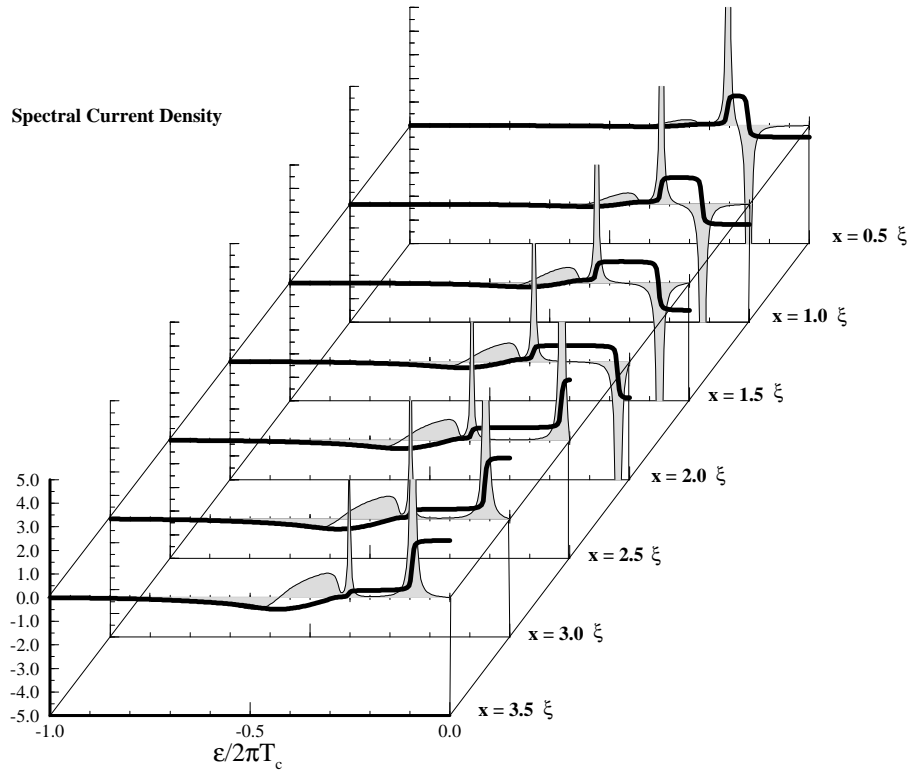


FIG. 4. The spectral current density of the 4π vortex for impact parameters, $x = 0.5\xi_0, \dots, 3.5\xi_0$. The cumulative spectral weight is shown as the thick solid line in each panel. Note the appearance of the *counter-moving* bound state at $x = 2.0\xi_0$ and the corresponding reversal in the integrated spectral weight for $x < 2\xi_0$.

C. Spectrum of a pinned s-wave vortex in a transport current

Finally, consider the current and excitation spectrum of a 2π vortex in the presence of a uniform supercurrent $\mathbf{j}_{tr} = j_{tr}\hat{\mathbf{x}}$. In the absence of pinning the vortex will move in the direction $(-\hat{\mathbf{y}})$ in order to reduce the kinetic energy. Thus, in order to investigate the excitation spectrum in the presence of a transport current we must pin the vortex to the lattice. Our model for the pinning center is a normal metal inclusion where the pairing interaction (or the local T_c) vanishes.

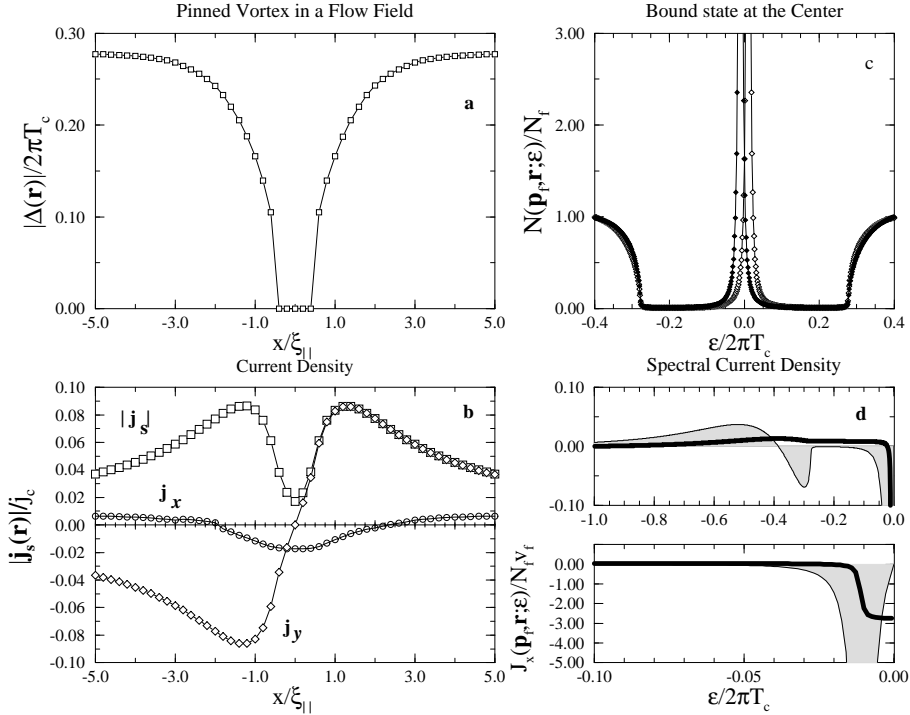


FIG. 5. *a*) The amplitude of the order parameter for a pinned 2π vortex at $T = 0.4T_c$. The normal inclusion has a diameter of $0.4\xi_0$, and the imposed transport current corresponds to $\mathbf{p}_s = 0.02\xi_0^{-1}(1, 0)$. The dotted curve corresponds to $|\Delta(x)|$ in the absence of the normal inclusion. *b*) Current density of the pinned vortex for a trajectory passing through the center of the core. *c*) The bound state spectrum at the center of the core of the pinned vortex in a uniform flow field. The two nearly zero-energy bound states correspond to co-moving and counter-moving trajectories. *d*) The spectral current density for a trajectory through the core. The negative energy counter-moving bound state carries the backflow current in the core. The thick line is the cumulative spectral weight for the current density. Note the scale changes for the two panels.

Fig. 5a shows the order parameter of a pinned vortex for an s -wave superconductor and a pinning center with a radius of $0.4\xi_0$. In the presence of a transport current the amplitude of the order parameter deforms; it is suppressed on the high current side of the vortex as shown in Fig. 5a. For relatively small transport currents, e.g. $\mathbf{p}_s = 0.02\xi_0^{-1}(1, 0)$, the center for the phase winding lies within the normal inclusion. However, as shown in Fig. 5b, the vortex current no longer vanishes at the center of the vortex core; there is substantial current *through* the vortex core region, including the normal inclusion. The current density inside the normal inclusion is carried by the Andreev bound states and is a consequence of the proximity effect. The bound state spectrum at the center of the vortex is shown for a trajectory parallel to the transport current and passing through the vortex center. The negative energy bound state carries the transport current inside the normal inclusion. Fig. 5d shows the spectral current density measured at the center of

the normal inclusion for the trajectories with $\mathbf{v}_f \parallel \mathbf{p}_s$. Note that the bound state dominates the current and that this current is opposite to the applied transport current. This result was also obtained in section II, without taking into account the distortion of the vortex core order parameter. This led to a violation of charge conservation in the core. Our numerical calculation shows that the main features of the analytic model for the bound state spectrum and the self-consistent determination of the order parameter for the pinned vortex in the presence of a transport current guarantees that charge is conserved.

CONCLUSIONS

We have discussed the current carried by the excitations of s-wave vortices in clean layered superconductors. The *spectral current density* was introduced in order to identify the excitations that determine the transport and circulating currents of a vortex. The bound states of the vortex carry most of the current in the vicinity of the core, including transport currents that flow through the core of a pinned vortex. Far from the vortex core currents are carried primarily by the bound-pair continuum that forms the condensate. For currents flowing through a pinned vortex, current conservation is maintained by “spectral transfer” of the current carried by the Andreev bound states to the continuum states outside the core. A novel example of the evolution of the spectral current density is provided by the double quantum vortex which shows the connection between the spectrum of bound states and the symmetry or topology of the order parameter. At low temperatures ($T = 0.4T_c$) the double quantum vortex exhibits a ‘current reversal’ relative to the asymptotic direction of the circulation. The counter-circulating current in the core is due to a counter-moving bound state that appears below the Fermi level and dominates the current for distances of order $0 < r \lesssim 2\xi_0$. At high temperatures, $T \rightarrow T_c$, this counter-moving bound state is thermally depopulated with the result that the current reversal in the core disappears in the Ginzburg-Landau limit. In summary, we find that the Andreev bound states dominate the current of vortices on the scale of a few coherence lengths. The nonequilibrium properties of vortices on this scale are expected to be dominated by the spectral evolution and dynamics of these bound states.

ACKNOWLEDGEMENTS

This work was initiated when the authors were participants at a workshop at the Institute for Scientific Interchange, Villa Gualino, Torino. The research of DW was supported in part by the Engineering and Physical Sciences Research Council, while that of DR and JAS was supported in part by NSF grant DMR 91-20000 through the Science and Technology Center for Superconductivity, the Max Planck Gesellschaft and the Alexander von Humboldt Stiftung. We also thank Dr. M. J. Graf for his comments on the manuscript.

IV. APPENDIX

A. A matrix element

In this appendix we derive a form for a matrix element used in section IID. The matrix element in question is $\langle \zeta | [iv_f \hat{p}_\zeta, \delta(\epsilon - \hat{H}_A)] | \zeta \rangle_{1,1}$ where we write

$$\hat{H}_A = v_f \hat{p}_\zeta \hat{\tau}_3 + \hat{\Delta}, \quad \hat{\Delta} \equiv \Delta_0 \frac{F(\hat{r})}{\hat{r}} (\hat{\tau}_1 \hat{\zeta} + \hat{\tau}_2 \eta). \quad (44)$$

We have

$$[iv_f \hat{p}_\zeta, \delta(\epsilon - \hat{H}_A)] = i \left(\hat{\tau}_3 (\hat{H}_A - \hat{\Delta}) \delta(\epsilon - \hat{H}_A) - \delta(\epsilon - \hat{H}_A) (\hat{H}_A - \hat{\Delta}) \hat{\tau}_3 \right) \quad (45)$$

$$= i [\hat{\tau}_3 \epsilon, \delta(\epsilon - \hat{H}_A)] - i \{ \hat{\tau}_3 \hat{\Delta}, \delta(\epsilon - \hat{H}_A) \}. \quad (46)$$

Then

$$\langle \zeta | [iv_f \hat{p}_\zeta, \delta(\epsilon - \hat{H}_A)] | \zeta \rangle_{1,1} = i \text{Tr} \left[\frac{1}{2} (1 + \hat{\tau}_3) \langle \zeta | ([\hat{\tau}_3 \epsilon, \delta(\epsilon - \hat{H}_A)] - \{ \hat{\tau}_3 \hat{\Delta}, \delta(\epsilon - \hat{H}_A) \}) | \zeta \rangle \right] \quad (47)$$

$$= -\text{Tr} \left[i \langle \zeta | \hat{\tau}_3 \hat{\Delta} \delta(\epsilon - \hat{H}_A) | \zeta \rangle \right]. \quad (48)$$

Substituting the explicit form for $\hat{\Delta}$ yields the relation

$$\langle \zeta | [iv_f \hat{p}_\zeta, \delta(\epsilon - \hat{H}_A)] | \zeta \rangle_{1,1} = \Delta_0 \frac{F(r)}{r} \text{Tr} \left[(\zeta \hat{\tau}_2 - \eta \hat{\tau}_1) \langle \zeta | \delta(\epsilon - \hat{H}_A) | \zeta \rangle \right]. \quad (49)$$

B. Approximation of bound states at large distances

Equation (12) gives the current density in terms of the Andreev Hamiltonian (8) whose eigenvalue equation reads

$$\left[-iv_f \partial_\zeta \hat{\tau}_3 + \Delta_0 \frac{F(\sqrt{\zeta^2 + \eta^2})}{\sqrt{\zeta^2 + \eta^2}} (\hat{\tau}_1 \zeta + \sigma^2 \eta) \right] \psi(\zeta) = E \psi(\zeta). \quad (50)$$

The parameter η appearing in the above equation has the semiclassical interpretation as a c-number impact parameter. In this appendix we present approximations to the above equation for large values of the impact parameter, η .

For $|\eta| \gg \xi_0$ we are justified to replace $F(\sqrt{\zeta^2 + \eta^2})$ by its asymptotic value of unity. Furthermore, making the somewhat crude approximation

$$\frac{(\hat{\tau}_1 \zeta + \hat{\tau}_2 \eta)}{\sqrt{\zeta^2 + \eta^2}} \rightarrow \hat{\tau}_1 \frac{\zeta}{|\eta|} + \hat{\tau}_2 \text{sign}(\eta) \quad (51)$$

yields for the bound state

$$\psi_0(\zeta) \simeq \text{constant} \times \exp \left(-\frac{\Delta_0}{2v_f |\eta|} \zeta^2 \right) \begin{pmatrix} \frac{1}{\sqrt{2}} \\ \frac{-i}{\sqrt{2}} \end{pmatrix}, \quad E_0 \simeq -\Delta_0 \text{sign}(\eta). \quad (52)$$

This indicates that at large impact parameters, the bound states of the Andreev equation are found very close to the threshold of the continuum.

When required, more refined estimates may be obtained by writing

$$\frac{(\hat{\tau}_1 \zeta + \hat{\tau}_2 \eta)}{\sqrt{\zeta^2 + \eta^2}} = \tau_1 \exp [i \arctan(\eta/\zeta) \hat{\tau}_3] \quad (53)$$

and then performing a unitary transformation $\hat{H}_A \rightarrow \hat{U} \hat{H}_A \hat{U}^{-1}$, $\psi \rightarrow \tilde{\psi} \equiv \hat{U} \psi$, with $\hat{U} = \exp \left[\frac{i}{2} \arctan(\eta/\zeta) \hat{\tau}_3 \right]$ to remove the phase from the order parameter. The transformed Andreev equation is

$$\left[-iv_f \partial_\zeta \hat{\tau}_3 + \frac{v_f}{2} \frac{\eta}{\zeta^2 + \eta^2} + \Delta_0 \hat{\tau}_1 \right] \tilde{\psi}(\zeta) = E \tilde{\psi}(\zeta), \quad (54)$$

This is a one dimensional Dirac equation with a weak scalar potential, which has weakly bound states with energies near $\pm \Delta_0$. A “non-relativistic” treatment is appropriate in this case and we approximate the Dirac equation by a Schrödinger equation. For example, for $\eta < 0$ we write

$$\tilde{\psi} = \psi_L \begin{pmatrix} 1 \\ 1 \end{pmatrix} + \psi_S \begin{pmatrix} 1 \\ -1 \end{pmatrix} \quad (55)$$

with $\psi_{L,S}$ scalars. Straightforward manipulations indicate that ψ_L approximately obeys the Schrödinger equation

$$\left[-\frac{v_f^2}{2\Delta_0} \frac{\partial^2}{\partial \zeta^2} - \frac{v_f}{2} \frac{|\eta|}{\zeta^2 + \eta^2} \right] \psi_L(\zeta) = (E - \Delta_0) \psi_L(\zeta). \quad (56)$$

All the machinery of Schrödinger theory may be used on this equation to estimate e.g. the bound states. We can put a lower limit on the bound state energy. This may be obtained from the fact that the eigenvalues of the Schrödinger operator are $\geq V_{\min}$, the minimum of the potential. Thus, $E - \Delta_0 \geq \text{Min}_\eta \left[-\frac{v_f}{2} \frac{|\eta|}{\zeta^2 + \eta^2} \right]$, i.e.

$$E \geq \Delta_0 - \frac{v_f}{2} \frac{1}{|\eta|}, \quad \eta < 0. \quad (57)$$

-
- ¹ J. Bardeen and M. J. Stephen, Phys. Rev. **140**, A1197 (1965).
- ² C. Caroli, P. G. deGennes, and J. Matricon, Phys. Lett. **9**, 307 (1964).
- ³ C. Caroli, P. G. deGennes, and J. Matricon, Phys. Kondens. Materie **3**, 380 (1965).
- ⁴ J. Bardeen, R. Kümmel, A. E. Jacobs, and L. Tewordt, Phys. Rev. **187**, 556 (1969).
- ⁵ L. Kramer and W. Pesch, Z. Phys. **269**, 59 (1974).
- ⁶ H. Hess *et al.*, Phys. Rev. Lett. **62**, 214 (1989).
- ⁷ C. Renner, A. D. Kent, P. Niedermann, and Ø. Fischer, Phys. Rev. Lett. **70**, 3135 (1991).
- ⁸ C. Renner and Ø. Fischer, Phys. Rev. B **51**, 9208 (1995).
- ⁹ I. Maggio-Aprile *et al.*, Phys. Rev. Lett. **75**, 2754 (1995).
- ¹⁰ J. Shore, M. Huang, A. Dorsey, and J. Sethna, Phys. Rev. Lett. **62**, 3089 (1989).
- ¹¹ U. Klein, Phys. Rev. B **40**, 6601 (1989).
- ¹² U. Klein, Phys. Rev. B **41**, 4819 (1990).
- ¹³ F. Gygi and M. Schluter, Phys. Rev. B **41**, 822 (1990).
- ¹⁴ F. Gygi and M. Schluter, Phys. Rev. Lett. **65**, 1820 (1990).
- ¹⁵ S. Ullah, A. Dorsey, and L. J. Buchholtz, Phys. Rev. B **42**, 9950 (1990).
- ¹⁶ B. Pöttinger and U. Klein, Phys. Rev. Lett. **70**, 2806 (1993).
- ¹⁷ A. F. Andreev, Sov. Phys. JETP **19**, 1228 (1964).
- ¹⁸ N. N. Bogolyubov, Tolmachev, and Shirkov, *New Methods in the Theory of Superconductivity* (Academy of Science, Moscow, 1958).
- ¹⁹ G. Eilenberger, Z. Physik **214**, 195 (1968).
- ²⁰ A. I. Larkin and Y. N. Ovchinnikov, Sov. Phys. JETP **28**, 1200 (1969).
- ²¹ D. Rainer and J. A. Sauls, in *Superconductivity: From Basic Physics to Latest Developments* (Singapore: World Scientific Publishers, 1995), pp. 45-78.
- ²² D. Waxman, Annals of Physics **223**, 129 (1993).
- ²³ We consider here only superconductors with a spin-singlet order parameter, and neglect the (typically) small Pauli paramagnetism.
- ²⁴ P. deGennes, *Superconductivity of Metals and Alloys* (W.H. Benjamin Inc., New York, NY, 1966).
- ²⁵ Note that the order parameter in (2) and (3) depends on $\hat{r} = \sqrt{\hat{\zeta}^2 + \eta^2}$.
- ²⁶ Note that $\hat{\mathbf{p}}_s \cdot \mathbf{j}_2(\mathbf{r}, T)$ is proportional to an (ϵ, φ) integral of $(\mathbf{q} \cdot \hat{\mathbf{k}}) [f(\epsilon + \mathbf{q} \cdot \hat{\mathbf{k}}) - f(\epsilon)] \langle \zeta | \delta(\epsilon - \hat{H}_A) | \zeta \rangle_{1,1}$. Since $\langle \zeta | \delta(\epsilon - \hat{H}_A) | \zeta \rangle_{1,1} \geq 0$ and $(\mathbf{q} \cdot \hat{\mathbf{k}}) [f(\epsilon + \mathbf{q} \cdot \hat{\mathbf{k}}) - f(\epsilon)] \leq 0$ it immediately follows that $\hat{\mathbf{p}}_s \cdot \mathbf{j}_2(\mathbf{r}, T) < 0$.
- ²⁷ A. Heeger, S. Kivelson, J. Schrieffer, and W.-P. Su, Rev. Mod. Phys. **60**, 781 (1988).
- ²⁸ M. Atiyah, V. Patodi, and I. Singer, Camb. Phil. Soc. **77**, 43 (1975).
- ²⁹ G. M. Eliashberg, Sov. Phys. JETP **34**, 668 (1972).
- ³⁰ A. Larkin and Y. Ovchinnikov, Sov. Phys.-JETP **41**, 960 (1976).
- ³¹ W. Pesch and L. Kramer, J. Low Temp. Phys. **15**, 367 (1974).
- ³² R. Watts-Tobin, L. Kramer, and W. Pesch, J. Low Temp. Phys. **17**, 71 (1974).
- ³³ E. Thuneberg, J. Kurkijärvi, and D. Rainer, Phys. Rev. **B29**, 3913 (1984).
- ³⁴ E. Thuneberg, J. Kurkijärvi, and J. A. Sauls, Physica **B+C:165-166**, 755 (1990).
- ³⁵ M. Fogelström and J. Kurkijärvi, J. Low Temp. Phys. **98**, 195 (1995).
- ³⁶ N. Schopohl and K. Maki, Physica **B 204**, 214 (1995).
- ³⁷ V. Hoffmann and D. Rainer, Molecular Physics Reports **11**, (1995).
- ³⁸ J. W. Serene and D. Rainer, Phys. Rep. **101**, 221 (1983).
- ³⁹ D. Rainer, in *Progress in Low Temperature Physics* (Elsevier Science Publishers B.V., 1986), Vol. 10, pp. 371-424.
- ⁴⁰ H. Eschrig, *Optimized LCAO Method and the Electronic Structure of Extended Systems, Sect. 7.4, Research Reports in Physics* (Springer-Verlag, Berlin, 1989).
- ⁴¹ N. B. Kopnin and V. E. Kratsov, Zh. Eksp. Teor. Fiz. **71**, 1645 (1976) [Sov. Phys. JETP, **44**, 861 (1976)].
- ⁴² For a recent review see N. Kopnin, *Theory of Flux Flow Hall Effect in Clean Type II Superconductors*, to be published in "Quasiclassical Methods in the theory of Superconductivity and Superfluidity", eds. D. Rainer and J. A. Sauls, Springer-Verlag, 1996.